Optoelectronic properties of Mg and Cu co-doped ZnO nanostructure

A. Ullah[a], N. Ali[b,*], A. A. A. Bahajjaj[c], A. Shahid[a], Q. S. Ahmad[a], M. Jabeen[d], M. Khan[a], A. Khesro[a,e]
[a]*Department of Physics, Abdul Wali Khan University Mardan, 23200, Pakistan*
[b]*African Sustainable Agriculture Research Institute (ASARI) Mohammad VI Polytechnic University (UM6P), Laayoune, Morocco*
[c]*Department of Chemistry, College of Science, King Saud University, Riyadh 11451, Saudi Arabia*
[d]*Government Graduate college for women south City okara, Pakistan*
[e]*Department of Materials Science and Engineering, the University of Sheffield Sir Robert Hadfield Building, Mappin Street, Sheffield, S1 3JD, UK*

In this work, both pure and Mg-Cu co-doped zinc oxide thin films are prepared by sol-gel spin coating technique. Microscopic glass substrates are used for the synthesis of thin films. The thin films are examined by X-ray spectroscopy (XRD), photoluminescence spectroscopy (PL), scanning electron microscopy (SEM), ultraviolet-visible spectroscopy (UV-Vis), and energy dispersive X-ray analysis (EDX). The XRD reveals the hexagonal wurtzite phase of the films. The observed grain size is 23.34 nm to 15.94 nm for pure and Mg-Cu co-doped ZnO respectively. The SEM image shows an increase in grain size and a smoothing of the surface with Mg-Cu co-doping. The presence of Mg and Cu in the ZnO nanofilm is confirmed by EDX analysis. UV analysis shows an increase in percent transmittance with doping. The Tauc relation is used to estimate the band gap of the samples, and a significant shift in the band gap is observed. The photoluminescence diagram shows greater emission and surface defects with doping. The visible spectrum is completely covered by the low- level emission.

(Received July 1, 2024; Accepted October 8, 2024)

Keywords: doping; transmittance; nanoparticles; photoluminescence

1. Introduction

Nano materials have the potential to revolutionize the field of energy by improving the efficiency of energy conversion, storage, and transmission. Nano materials can be designed to have unique and often unexpected properties that are not seen in bulk materials, which makes them particularly promising for energy applications. In the present era, where Nano-sciences had made a great improvement to comfort mankind for energy production and distribution. The modern progress in technology, ultimately requests more efficient physical as well as chemical techniques for the development and production of advanced systems, and inter-conversion of different forms of energy. In spite the fact that worldwide, fossil assets have not been depleted but the destructive health, social and ecological effects of our currently used inappropriate pattern of different forms of energy is evident [1, 2].Large scale alternative of energy production is required to sustain and improve our life standardin future due to population growth and globalization. [3, 4]. It appears quite likely that greenhouse gas emissions will increase and will result into considerable global warming in future in the next 5 decades. The connection between energy and climate change highlights the urgent need to transition to a more sustainable and resilient energy system that can support economic development and improve the well-being of people and the planet. This requires a concerted effort from governments, businesses, and individuals to prioritize and invest in clean energy technologies and practices, as well as to reduce greenhouse gas emissions in all sectors of the economy.Wind,

* Corresponding author: nisaraliswati@hotmail.com
https://doi.org/10.15251/DJNB.2024.194.1449

geothermal, solar energy and biomass are just a few among sustainable energy resources that have emerged as a result of scientific and technological advancements [5, 6].

Solar energy is a very clean and green source of energy and nano materials such as nanowires, quantum dots, and nanostructured surfaces can be used to improve the light absorption and charge transport in solar cells, resulting in higher energy conversion efficiencies. This will not only be free energy but will reduce carbon dioxide (CO_2) emissions. Different materials have been utilized for the production of solar energy and among them ZnO is viable material due to its magic nature. The tunable bandgap, superior optical properties and excellent electrical and structural properties make it very distinct material in photovoltaics.Zinc oxide (ZnO) is a versatile inorganic compound that is widely used in various industries due to its unique properties. It is a white or yellowish powder that is insoluble in water and is often found in nature as the mineral zincite. One of the most significant properties of ZnO is its semiconducting behavior, which makes it useful for applications in electronics and optoelectronics. ZnO has a wide bandgap, which allows it to absorb and emit light in the ultraviolet region of the spectrum. This property makes it useful for developing ultraviolet (UV) detectors, light-emitting diodes (LEDs), and other optoelectronic devices.ZnO also exhibits piezoelectric propertieswhich makes it useful for energy harvesting and sensing applications.ZnO is a good conductor of electricity and has good thermal stability, which makes it useful for developing electrodes and other conductive materials.ZnO is also used in a variety of other applications. For example, it is widely used as a white pigment in paints, plastics, and ceramics due to its high reflectivity and opacity. It is also used as a food additive and in cosmetics due to its antimicrobial and anti-inflammatory properties.ZnO is a semiconducting combination made up of $_{30}$Zn and $_{8}$O. Zinc has a number of stable isotopes, the most common of which are ^{64}Zn (48.89%) and ^{68}Zn (18.57%), on the other hand oxygen is nearly made up entirely of the isotope ^{16}O. (99.76%).The hexagonal wurtzite structure is ZnO's characteristic crystal structure. The sp^3 hybridization of the electron states in ZnO's crystal lattice results in four similar orbitals oriented in tetrahedral topology. The valence band in the resultant semiconducting crystal is made up of bonding sp^3 states, whereas the conduction band is made up of its antibonding match. The resultant energy band is 3.4 eV, which is in the ultra violet spectral range. Due to these propertied scientist aregetting attention in ZnO as a transparent electronic compounds[7].The piezoelectric effect is exceptionally strong for ZnO with tetrahedrally coordinated atoms which creates an electrical polarization that results in the generation of a voltage across the material. When compared to other II-VI composites with wurtzite morphology, the ZnO piezoelectric tensor coefficients are almost double. ZnO is therefore widely used for electromechanical coupling operations and has been for a long time. Three main features affect the vibration dynamics of the ZnO lattice: (1) the uniaxial grain structure, (2) the large mass variance between the oxygen and zinc ions and (3) the strong bonding polarization. The vibration eigenmodes are classified according to their symmetry by the uniaxial structure. The significant mass difference reflects in the oxygen-dominated modes having much higher frequencies than the zinc-dominated modes. In the Near-ultraviolet and visible ranges, ZnO is a broad gap semiconductor with good optical transparency and luminous character. ZnO is a potential compound for electrical and photonic applications like solar cells because of their express qualities [8].

2. Experimental

Sol gel technique is employed for the synthesis of pure and doped ZnO. Spin coater is used to deposit the prepared solution on a microscopic glass slides pre cleaned ultrasonically[9].The list of the chemicals, chemical formula, molecular weight along with purity percentage are given in the Table 1.Two different solutions were prepared for pure Zinc Oxideand Copper-Magnesium co-doped Zinc Oxide.Pure zinc oxide solution was produced by taking 1.317g of zinc acetate dihydrate in 20ml of 2-methoxy ethanol. The solution was kept on a hot plate stirrer for 45 minutes and temperature was kept constant at 65 degrees Celsius ($\pm 5^0$C). A cloudy solution was obtained after constant stirring. Keeping the molar ratio of zinc acetate to mono ethanolamine at 1:1, 0.362ml of mono ethanolamine (MEA) was added to the prepared solution.

Table 1. List of Chemicals used.

S No	Name	Chemical formula	Molecular weight	Purity	Company name
1	Zinc acetate dihydrate	Zn $(CH_3COO)_2.2H_2O$	219.51g/mol	99%	SIGMA ALDRICH
2	2-Methoxy ethanol	$C_3H_8O_2$	76.10g/mol	99%	SIGMA ALDRICH
3	Mono ethanolamine	C_2H_7NO	61.08g/mol	98%	SIGMA ALDRICH
4	Magnesium acetate tetra hydrate	Mg $(CH_3COO)_2.4H_2O)$	214.46g/mol	99%	SIGMA ALDRICH
5	Copper acetate dihydrate	Cu $(CH_3COO)_2.2H_2O$	181.63g/m	99%	SIGMA ALDRICH

The cloud like solution turns completely clear by the drop wise addition of MEA. The reaction indicated the formation of zinc oxide. Then the solution was kept for stirring further for 1 hour and 30 minutes. The desired solution was prepared and kept for aging at room temperature for 24 hours. Zinc oxide is doped with copper and magnesium, synthesized by taking 1.198g of zinc acetate dihydrate in 20ml of 2-methoxy ethanol. 0.09g (7 wt.%) of magnesium acetate tetrahydrate and 0.02611g (2 wt.%) of copper acetate dihydrate was added to the solution and agitated continuously for 1 hour. The temperature was kept constant at 65 degrees Celsius ($\pm5^0$C). Hence a bluish cloudy solution was prepared. After addition of MEA dropwise the solution turned transparent. The quantity of MEA was considered such that the molar ratio of mono ethanolamine to zinc source is 1:1. 0.35ml of MEA was added drop wise to the solution. Finally, the solution was further agitated for 2 hours. The desired solution was ready and kept for aging at room temperature[10, 11].Using simple glass as substrate, all the solutions were deposited on it through spin coater. First of all, the glass substrates were dipped in a mixture of De-ionized water and ammonia. The solution having glass substrates was kept in sonicator for 1 hour at 50^0C. Then the glasses were kept in oven for 30 minutes at 60^0C to dry[12].

The spin coater was cleaned with ethanol and the aged solutions were filled in a dropper. The speed of rotor was set to 2500rpm for a total of 90 seconds. The solutions were applied to the pre-cleaned glass by addition of solution drops from dropper. To get uniform distribution the drops were added to the glass after the glass gained some speed on spin coater. Then the glass was dried on hotplate for 10 minutes. The temperature of hotplate was kept at 200^0C. This process was repeated four times to attain the required thickness. Finally, the deposited samples were annealed at 550^0C, and the desired samples were ready for characterization.

3. Results and discussion

3.1. X-ray diffraction

X-Ray diffraction technique was used to examine the crystal structure of the prepared samples. The XRD spectroscopy was performed in the range of 30^o to 60^o at 2θ angle. The XRD pattern of ZnO and Mg-Cu co-doped ZnOare demonstrated in Figure 1. All the peaks were in correspondence to polycrystalline structure matched with (JCPDS-79-0206). The strong diffraction peak from (002) associate to the hexagonal wurtzite structure. These diffraction peaks are observed at 2θ angle 31.7°, 34.3°, and 36.2°, which are indexed to (100), (002) and (101) respectively. Peak intensity of Mg-Cu co-doped ZnOhas increased. Table 2 shows that FWHM also increases with addition of dopant. Using Scherrer equation, the average crystallite size for pure and Mg-Cu co-doped ZnOis calculated to be 23.38 and 15.94 nm respectively.XRD patterns were examined to calculate peak intensity, FWHM, position and width, data was used with the Scherer formula[13, 14]. The typical XRD pattern exhibit that the sample contains single phase wurtzite structures.

$$D = k\lambda/\beta\cos\theta$$

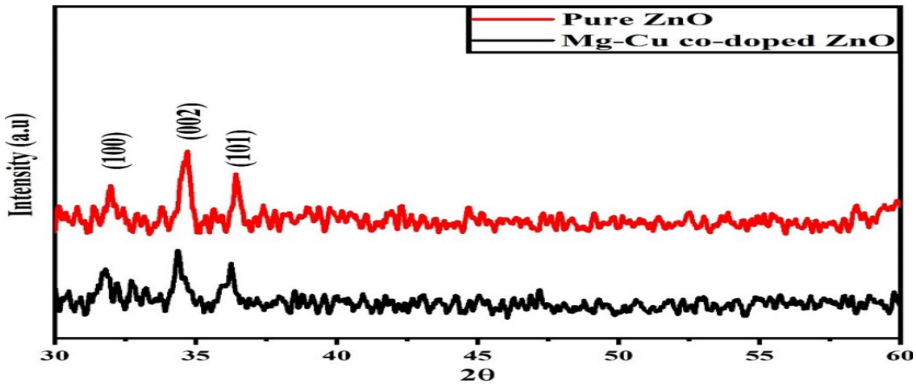

Fig. 1. XRD spectrum of pure and co-doped ZnO.

Table 2. Lattice parameters of Pure and Mg-Cu do-doped ZnO.

Pure ZnO					
S No	**2θ**	**FWHM**	**Crystallite size (nm)**	**Miller Indices (*hkl*)**	**Micro strain**
1	31.97662	0.32114	25.73318824	100	4.89E-03
2	34.63391	0.37137	22.40751458	002	5.20E-03
3	36.45158	0.38016	22.00098419	101	5.04E-03
Average crystallite size = 23.38 nm					
Mg-Cu co-doped ZnO					
1	31.78919	0.60635	13.62265363	100	9.29E-03
2	34.41366	0.46402	17.9227408	002	6.54E-03
3	36.18894	0.51388	16.26373587	101	6.86E-03
Average crystallite size = 15.94 nm					

3.2. Scanning electron microscopy

SEM images of co-doped ZnO can reveal important information about the material's microstructure and surface morphology. The SEM images show the presence of nanoparticles or other structural features that can affect the material's properties. The exact appearance of co-doped ZnO in an SEM imagedepend on a variety of factors, such as the specific doping concentrations and the synthesis method used to create the material. The co-doped ZnO appear as a rough, granular surface with distinct features that can be analyzed to gain insight into the material's properties and behavior. Figure 2 shows a specific SEM image of pure ZnO and Mg-Cu co-doped thin films that were applied onto the glass by using the sol-gel spin coating technique. It was found that the grain size of Mg-Cu co-doped ZnO is smaller than that of undoped ZnO. Crystalline microstructures of nanoscale order with homogeneous and dense distribution are present in both the pure and Mg-Cu co-doped ZnO films. Precursor solution doping has a minor impact on the surface of the porous microstructure. With the addition of dopants, the surface uniformity and roughness have reduced. The pure and Mg-Cu co-doped thin films were annealed at 550 ^{0}C and both had flatter surfaces and uniform grain sizes. By adding Mg and Cu, the grain size also grew denser and bigger. This result may be explained by the fact that thin films relieve stress by increasing their particles size and creating micropores or fractures in order to prevent slipping off the quartz substrates at higher annealing temperatures.

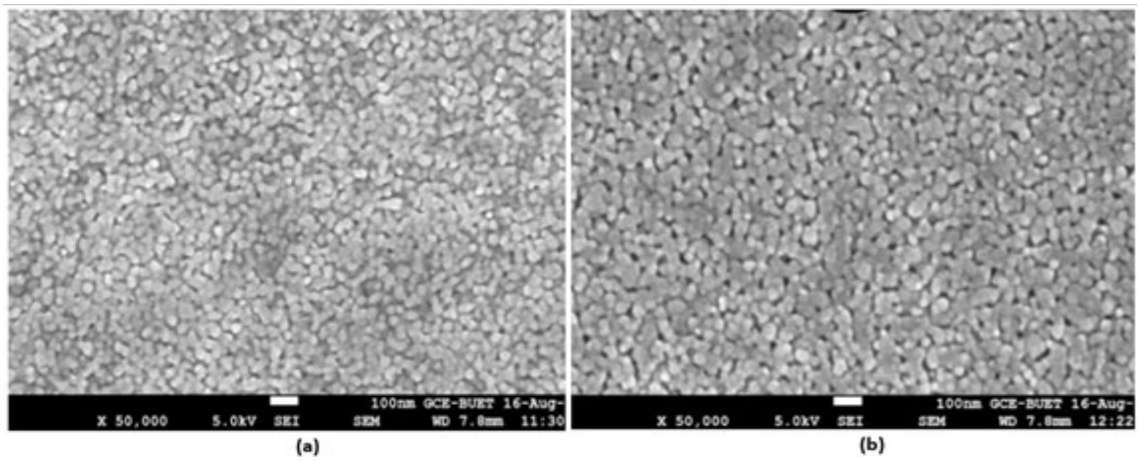

Fig. 2. SEM images of (a) Mg-Cu co-doped ZnO (b) Pure ZnO.

3.3. Energy dispersive X-ray spectroscopy

To confirm the incorporation of dopants in the ZnO thin Film, it is required to analyze the sample using EDS. The EDS spectra from a sample of Mg-Cu co-doped ZnO films is shown in Figure 3. The magnesium is shown by the peak at 1.25 KeV. Two more peaks positioning at 1.012 and 0.525 keV, respectively confirm the existence of Zinc and Oxygen. The 1.51 keV peak indicates the presence of copper. While a peak at 1.74 keV reveals the presence of silicon for the films grown on a silicon substrate.

3.4. UV-visible spectroscopy

UV-Visible spectroscopy is a useful technique for characterizing the electronic properties of materials, including chalcogenides, ZnO etc. In UV-Visible spectroscopy, a sample is irradiated with light in the UV-Visible region of the electromagnetic spectrum, and the transmitted or reflected light is measured as a function of wavelength. For ZnO, the UV-Visible spectrum typically shows a sharp absorption edge in the UV region, which corresponds to the band gap energy of the material [15]. The exact position of the absorption edge depends on the specific properties of the ZnO sample, such as its crystal structure, morphology, and doping concentration. Absorbance and percentage transmission of the sample were calculated in the range of 250-800 nm via UV-Vis spectroscopy. Figure 4 (a) represents the absorption coefficient indicating the absorption property of the samples.

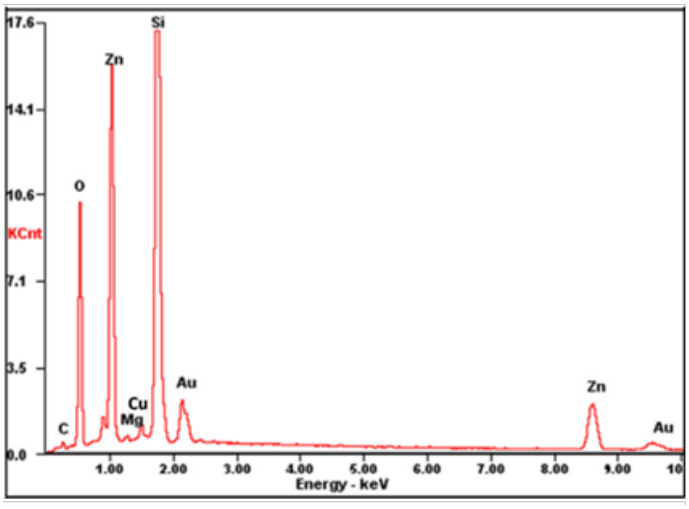

Fig. 3. EDX analysis of of pure and Mg-Cu co-doped ZnO.

Absorption coefficient α is defined as

$$\alpha = (2.303 \times A)/t$$

where, "A" represents absorbance and "t" represents thickness of the film[16].

Both the samples display a greater uniform transmittance (85%-90%) in visible range (Figure 4 (b)). Due to surface smoothing property and less defect of Mg, the transmittance of the film increased. However, both the samples experience a strong cut-off at ultraviolet region of light with a wavelength of around 375-380 nm, exhibiting significant UV light absorption that suggests the application of ZnO and Mg-Cu co-doped ZnO in UV detection. The material has a direct band gap due to the sharp-edged absorption.

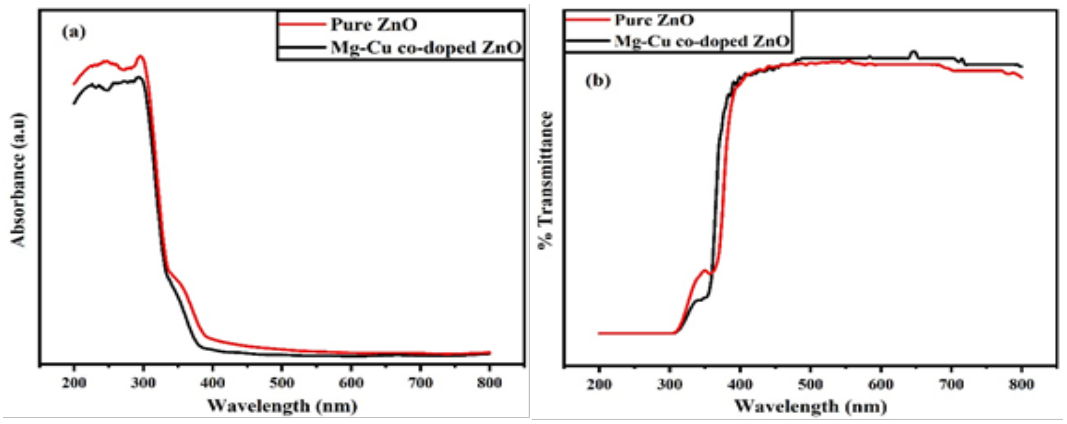

Fig. 4. (a) Absorption spectra of pure and Mg-Cu co-doped ZnO (b) Percentage transmission of pure and Mg-Cu co-doped ZnO.

The effect of Co doping on the band gap of ZnO can also depend on the concentration of the dopant. At low concentrations, the Co dopants may only introduce localized states in the band gap, which do not significantly affect the overall band gap energy. At higher concentrations, on the other hand, the Co dopants may have a more significant effect on the band gap[17]. The introduction of dopants into the ZnO crystal lattice will lead to changes in the electronic band structure, which can affect the band gap energy. The co-doping may lead to an increase in the band gap energy of ZnO. This can occur because the Co dopants introduce new energy levels into the band structure, which can overlap with the valence or conduction bands and enhance the effective band gap energy.Tauc relation was used to estimate optical band gap of the samples[18].

$$(\alpha h\nu)^{1/n} = A(h\nu - E_g)$$

where:

α = Absorption coefficient
h = Plank constant
ν = Frequency of radiation
E_g=Band gap energy

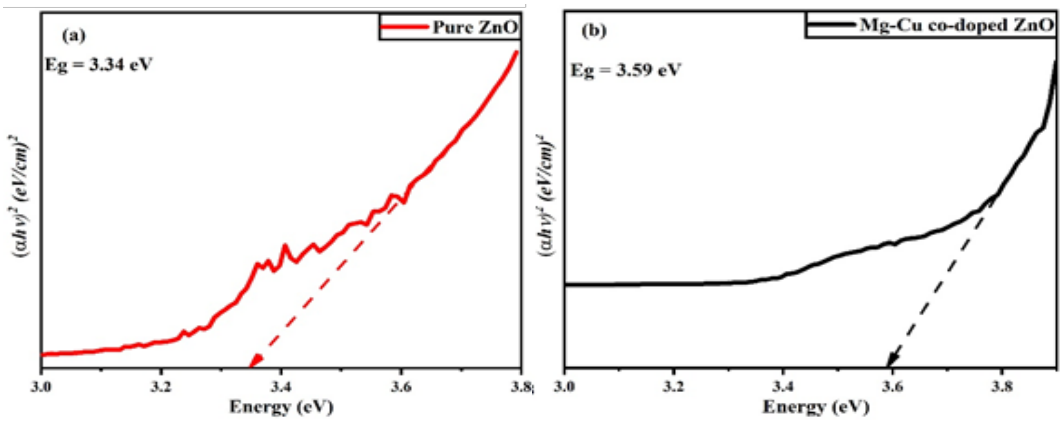

Fig.5. (a) Tauc plot of pure ZnO (b) Tauc plot of Mg-Cu co-doped ZnO.

As ZnO undergo direct transition, the "n" value is taken 2 to draw the plot between $(\alpha hv)^2$ and hv fig. By extending the linear part of the graph to the x-axis optical band gap of the samples was determined. The value of band gap for ZnO and Mg-Cu co-doped ZnO was found to be 3.34 eV and 3.59 eV respectively (Figure 5). The increase in band gap energy is due to the Mg doping.

3.5. Photoluminescence

Figure 6 shows the PL intensity vs wavelength plot of pure and Mg-Cu doped ZnO. Due to deep level defects (DLE) and band to band emission (BBE), ZnO emits two different types of emissions: UV and visible. Usually, ZnO possess six types of defects, three oxygen based and three zinc related. The visible spectrum is thoroughly covered by the deep level emission produced by ZnO. The concentration of the relevant defect affects how strong the DLE is. The Green emission in ZnO is often caused by V_o and $O_i$related defects. The PL plot–curve of samples indicates band-to-band emission at 358 nm. The deep level emission at 430 nm is due to V_{zn}. The graph indicates oxygen defect peaks at 536 nm and 574 nm for Mg-Cu ZnO, these peaks are not observed in pure ZnO. The peaks 430 nm, 451 nm and 465 nm may represent the emission from Zinc based defects. The emission peaks found at 358 nm, 430 nm, 451 nm, 465 nm, 536 nm and 570 nm represents violet, blue and green emission respectively.

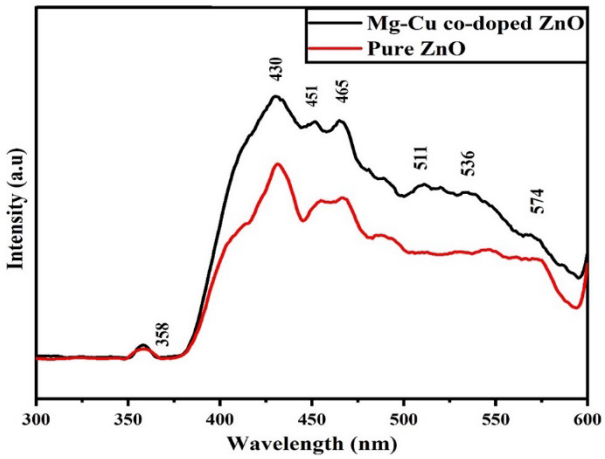

Fig. 6. PL spectra of co-doped ZnO.

4. Conclusion

Pure and Mg-Cu co-doped zinc oxide thin films were synthesized using sol-gel procedure on a microscopic glass through spin coating. The synthesized samples were characterized using various techniques to investigate optical and structural properties.X-ray diffraction pattern confirms hexagonal wurtzite structured ZnO thin films with good crystallinity. The crystallite size is observed to decrease while the surface smoothness tends to increase with Mg-Cu co-doping. The SEM image reveals that the grain size decreases due to Mg and Cu incorporation which gives a smoother surface to the thin film. EDX analysis represents the composition of elements of the thin film. The appearance of Mg and Cu in the ZnO is confirmed from the EDX results. UV-Visible spectroscopy is used to observe the transmittance and absorbance of the prepared samples. Both the films show significant absorbance in UV range and transmittance in visible range. The band gap of the doped sample increased because of the reduced grain size of the doped particles.PL spectra show the emission peaks in ultraviolet, blue and green region which are indexed as UV, blue and green emission. The intensity of defect peaks is observed to increase with Mg-Cu co-doping. From the above study Mg-Cu co-doped ZnO thin film can be considered as a sustainable candidate for window layer used in solar cell applications. The absorption property of UV spectra makes it a decent contestant to be used in UV detectors, light emitters and other photovoltaic devices.

Acknowledgments

This work was funded by the Researchers Supporting Project Number (RSPD2024R763) King Saud University, Riyadh, Saudi Arabia. The authors are also thankful to Abdul Wali Khan University of Science and Technology, Mardan, HEC Pakistan and HED for their kind support.

References

[1] Ranabhat, K., et al., An introduction to solar cell technology. 2016. 14(4): p. 481-491; https://doi.org/10.5937/jaes14-10879

[2] Ali, N., et al., A review on perovskite materials with solar cell prospective. 2021. 45(14): p. 19729-19745; https://doi.org/10.1002/er.7067

[3] Burton, I.J.E.S. and P.f.S. Development, Report on reports: Our common future: The world commission on environment and development. 1987. 29(5): p. 25-29; https://doi.org/10.1080/00139157.1987.9928891

[4] French, H.F.J.W.T., [BOOK REVIEW] Vanishing borders, protecting the planet in the age of globalization. 2000. 56(10): p. 26-27.

[5] Turner, J.A.J.S., A realizable renewable energy future. 1999. 285(5428): p. 687-689; https://doi.org/10.1126/science.285.5428.687

[6] Ali, N., et al., Advances in nanostructured homojunction solar cells and photovoltaic materials. 2020. 107: p. 104810; https://doi.org/10.1016/j.mssp.2019.104810

[7] Klingshirn, C.F., et al., Zinc oxide: from fundamental properties towards novel applications. 2010; https://doi.org/10.1007/978-3-642-10577-7

[8] Soosen Samuel, M., L. Bose, and K.J.A.R. George, Optical properties of ZnO nanoparticles. 2009. 16: p. 57-65.

[9] Ali, N., et al., A Study on Optoelectronic Properties of Copper Zinc Tin Sulfur Selenide: A Promising Thin-Film Material for Next Generation Solar Technology. 2021. 56(7): p. 2000159; https://doi.org/10.1002/crat.202000159

[10] Zhao, Z.-A., et al., Journal of Environmental Sciences, 2024. 136: p. 615-625; https://doi.org/10.1016/j.jes.2023.01.026

[11] Yang, D.-L., et al., Particuology, 2024. 85: p. 22-48; https://doi.org/10.1016/j.partic.2023.03.013

[12] V, D., V. B, A. Sebastian, Optical Materials, 2023. 138: p. 113646; https://doi.org/10.1016/j.optmat.2023.113646

[13] Ali, N., et al., Preparation and characterization of layer-diffusion processed InBi2Se4 thin films for photovoltaics application. 2020. 220: p. 164935; https://doi.org/10.1016/j.ijleo.2020.164935

[14] Ali, N., et al., Optoelectronic properties of thermally coated tin selenide thin films for photovoltaics. 2022. 46(3): p. 3725-3731; https://doi.org/10.1002/er.7402

[15] Tiwari, A., P.P. Sahay, Optical Materials, 2022. 134: p. 113098; https://doi.org/10.1016/j.optmat.2022.113098

[16] Shahzad, N., et al., Annealed tin selenide (SnSe) thin film material for solar cell application. 2020. 17(7): p. 347-351.

[17] Mohammed, L.H., et al., Chemical Engineering Journal Advances, 2023. 14: p. 100495; https://doi.org/10.1016/j.ceja.2023.100495

[18] Ul Haq, B., et al., Materials Science and Engineering: B, 2021. 265: p. 115043; https://doi.org/10.1016/j.mseb.2021.115043